

# Treatment with Stem Cells from Human Exfoliated Deciduous Teeth and Their Derived Conditioned Medium Improves Retinal Visual Function and Delays the Degeneration of Photoreceptors

Xiao-Xia Li,<sup>1</sup> Xiao-Jing Yuan,<sup>1</sup> Yue Zhai,<sup>1</sup> Shi Yu,<sup>1</sup> Rui-Xuan Jia,<sup>2</sup> Li-Ping Yang,<sup>2</sup>  
Zhi-Zhong Ma,<sup>2,3</sup> Yu-Ming Zhao,<sup>1</sup> Yi-Xiang Wang,<sup>4</sup> and Li-Hong Ge<sup>1</sup>

Retinitis pigmentosa (RP) is a hereditary disease characterized by degeneration and the loss of photoreceptors. Stem cell-based therapy has emerged as a promising strategy for treating RP. Stem cells from exfoliated deciduous teeth (SHEDs), a type of mesenchymal stem cell from human exfoliated deciduous teeth, have the potential to differentiate into photoreceptor-like cells under specific induction *in vitro*. It has been confirmed that through paracrine secretions, SHEDs exert neurotrophic, angiogenic, immunoregulatory, and antiapoptotic functions in injured tissues. This study was designed to determine whether retinal-differentiated SHEDs and the conditioned medium derived from SHEDs (SHEDs-CM) have therapeutic effects in a mouse model of RP. The results showed that both SHEDs and SHEDs-CM improved electroretinogram responses, ameliorated photoreceptor degeneration, and maintained the structure of the outer segments of photoreceptors. The therapeutic effects were related to antiapoptotic activity of SHEDs and SHEDs-CM. Thus, SHEDs may be a promising stem cell source for treating retinal degeneration.

**Keywords:** stem cells, exfoliated deciduous teeth, conditioned medium, stem cell therapy, retinal degeneration, retinitis pigmentosa

## Introduction

RETINITIS PIGMENTOSA (RP) is a hereditary disease characterized by degeneration and loss of photoreceptors. Inheritance can be autosomal dominant, autosomal recessive, or X-linked. RP has variable prevalence in different ethnic groups, and on a worldwide scale affects 1 in 4,000, involving a total of over 1 million individuals [1]. The age at onset of RP varies from infancy to late middle age with severe visual impairments detected by age 40–50. The photoreceptors, which send signals from the eye to the brain, are rods and cones. In the early stages of RP, rods degenerate and patients experience night blindness and progressive loss of the peripheral visual field; in later stages, patients develop tunnel vision and eventually experience severe visual impairment due to cone degeneration. The loss of rods and cones is accompanied by changes in the retinal pigment epithelial cells

and retinal glia; ultimately, the inner retinal neurons, blood vessels, and the optic nerve head are affected [2]. Some RP patients become blind as they age, ~25% becoming legally blind (20/200) and 0.5% becoming completely blind in both eyes [3]. Finding an effective and safe treatment for retinal degenerative diseases would greatly benefit patients and help reduce the economic burden on society.

A range of therapeutic strategies are used to treat RP, such as dietary supplementation with high doses of docosahexaenoic acid and vitamin A, physiotherapy with laser or surgical interventions with retinal prosthetic implantation, and intravitreal delivery of drugs or neurotrophic factors. So far, none of these has been ideal or effective. For example, a clinical trial reported that a large number of patients (11/30) experienced 23 serious adverse events after implantation of retinal prosthetics [4]. Gene therapy [5,6] and stem cell therapy [7] are emerging as promising strategies. As retinal tissue

<sup>1</sup>Department of Pediatric Dentistry, Peking University School and Hospital of Stomatology, National Engineering Laboratory for Digital and Material Technology of Stomatology, and Beijing Key Laboratory of Digital Stomatology, Beijing, China.

<sup>2</sup>Institute of Systems Biomedicine and Department of Ophthalmology, School of Basic Medical Sciences, Peking University Third Hospital, Beijing, China.

<sup>3</sup>Beijing Key Laboratory of Restoration of Damaged Ocular Nerve, Peking University Third Hospital, Beijing, China.

<sup>4</sup>Central Laboratory, Peking University School and Hospital of Stomatology, National Engineering Laboratory for Digital and Material Technology of Stomatology, and Beijing Key Laboratory of Digital Stomatology, Beijing, China.

has a limited ability to self-regenerate or self-repair, stem cell- or other cell-based therapy is attractive to clinicians and researchers for their potential for retinal regeneration and neuroprotection. Finding an ideal source of stem cells for transplantation is a key issue for this field.

Earlier, the transplantation of human photoreceptors [8], human fetal neuroretinal cells [9], or intact sheets of human fetal retina [10] in clinical trials to treat RP patients have achieved preliminary success. More recently, photoreceptors and tissue from neonatal retina [11], embryonic stem cells, or induced pluripotent stem cells [12–14] have been shown to repair retinal structure and visual function in animal models of retinal degeneration. However, the limited sources of neonatal retina, the ethical controversy, and the immunological rejection associated with embryonic stem cells and fetal grafts, or the risk of genetic mutations associated with induced pluripotent stem cells and their derived tissues prevent their further clinical application. Therefore, human adult stem cells without these concerns are emerging as a promising source.

Mesenchymal stem cells (MSCs) are adult stem cells isolated from many tissues, such as bone marrow and umbilical cord, as well as deciduous teeth. Stem cells from exfoliated deciduous teeth (SHEDs) possess characteristics typical of MSCs [15]; they express embryonic stem cell markers [16] and have immunomodulatory activity [17]. Theoretically, since they originate from the neural crest, SHEDs are likely to have a better capacity for neural differentiation than other kinds of MSCs. It has been confirmed that SHEDs secrete neurotrophic factors, cytokines, and chemokines which favor neural repair [18–20], regulate angiogenesis [21], and resist inflammation [22]. Based on this, we hypothesized that SHEDs can be used to treat retinal degeneration. In a previous study, we confirmed that conditioned medium derived from SHEDs (SHEDs-CM) have the potential to differentiate into photoreceptor-like cells and maintain good viability *in vivo* in mice with retinal degeneration [23]. However, whether SHEDs or their secretions (SHEDs-CM) are effective in preserving or restoring photoreceptors, retinal structure, and visual function was largely unknown.

Therefore, we set out to determine whether SHEDs and SHEDs-CM could be used to treat RP in a mouse model.

## Materials and Methods

### *SHED culture and retinal induction*

SHEDs were a gift from the Oral Stem Cell Bank of Beijing, Tason Biotech Co. Ltd. The culture medium was alpha-modified Eagle's minimum essential medium (Gibco BRL) supplemented with 10% fetal bovine serum (Gibco BRL), 1% penicillin/streptomycin, and 2 mM glutamine. SHEDs were identified by flow cytometry as we previously reported [23]. Differentiation toward a retinal fate was accomplished using our previously published protocols [23]. In brief, SHEDs at passages 3–5 were selected for two-step induction. In step one, floating culture ( $2 \times 10^5$  cells/mL) in a low-attachment dish (Nest) for 3 days was carried out to obtain neuron-like spheres in Medium 1, Dulbecco's modified Eagle's medium (DMEM)/F12 with several supplements (Supplementary Table S1). In step 2, the neurospheres were collected

and dissociated by 3 min of accutase incubation (STEMCELL Technologies) at 37°C. The cell suspension was then transferred to dishes or coverslips coated with Matrigel (Corning) at  $2 \times 10^4$  cells/cm<sup>2</sup>. In step 2, during the previous 7 days (days 3–10), cells were treated with Medium 2 (Supplementary Table S2) for mid-stage induction. During the final 14 days of induction, the culture medium was switched to Medium 3 (Supplementary Table S3) for final-stage photoreceptor induction. The medium was changed every 3 days.

### *Real-time reverse transcription-polymerase chain reaction analysis*

Total mRNA was extracted using TRIzol reagent (Invitrogen) according to the manufacturer's instructions. Total RNA was converted to cDNA using a reverse transcriptase kit (Promega). *GAPDH* was used as an internal control. The primer sequences are listed in Supplementary Table S4. The quantitative polymerase chain reaction was carried out in triplicate in 96-well plates using a 7900HT Fast Real-Time system (Applied Biosystems). The comparable cycle threshold method ( $2^{-\Delta\Delta C_T}$ ) was used to calculate the relative expression levels of the target genes.

### *Preparation of SHEDs-CM and CM-Dil- or green fluorescent protein-labeled SHEDs*

SHEDs-CM was collected by ultrafiltration. In brief, 80%–90% confluent SHEDs at passages 2–4 were washed thrice with phosphate-buffered saline (PBS) and were cultured in phenol red-free DMEM without serum for 48 h, and then the culture medium was collected and centrifuged at 726g for 5 min at 4°C to remove cell debris. Next, the supernatant was centrifuged in 3-kDa MW cutoff Amicon<sup>®</sup> Ultra-15 ultra-centrifuge tubes (Merck Millipore) at 3,200g for 45 min at 4°C and the supernatant was collected as SHEDs-CM. The protein concentration was measured as 700–900 µg/µL with a Pierce<sup>™</sup> BCA Protein Assay Kit (ThermoFisher Scientific) according to the manufacturer's instructions. We consistently obtained 500 µL of filtrate from 10 mL of primary culture medium. The filtrate was sterilized using 0.22 µm filters (Merck Millipore) and stored at –80°C before use.

Differentiated SHEDs at ~14 days were used for transplantation. All SHEDs were labeled with the cell membrane dye chloromethyl-benzamidodialkylcarbocyanine (CM-Dil; Invitrogen) 10–12 h before transplantation according to the manufacturer's instructions so they could be identified in histological examination. Undifferentiated SHEDs were marked with green fluorescent protein (GFP) by transfection of lentiviral vectors carrying the GFP gene according to the manufacturer's instructions.

### *Animals and subretinal injection of SHEDs and SHEDs-CM*

We used the well-established model of slow retinal degeneration, C57/BL6J mice with RPGR knockout, a kind gift from Prof. Yang Liping (Peking University Third Hospital). These mice slowly undergo retinal degeneration from the age of 2 months, have a substantial decrease of photoreceptors and their biomarkers rhodopsin and opsin at 6 months, and show a significant reduction of outer nuclear layer (ONL)

thickness and loss of rhodopsin and opsin expression at 12 months [20,21]. This study was approved by the Laboratory Animal Welfare Ethics Branch of the Biomedical Ethics Committee of Peking University (LA2018240). All surgical interventions and animal care were in accord with the Guide for the Care and Use of Animals of Peking University Health Science Center. Animals were housed in a regulated environment ( $22\pm 2^\circ\text{C}$ ,  $55\pm 5\%$  humidity, and a 12-h light:12-h dark cycle) with ad libitum food and water.

A cell suspension ( $2\times 10^4$  cells/ $\mu\text{L}$ ) or SHEDs-CM were injected into the subretinal space of  $\sim 4$ -month-old mice in the experimental group ( $n=12$ ), and balanced medium was injected in the control group ( $n=12$ ) under an ophthalmic operating microscope (Topcon). The pupils were dilated with 1% tropicamide 30 min before treatment. Ketamine (100 mg/kg) and xylazine (10 mg/kg; Sigma-Aldrich) were injected intraperitoneal (i.p.) for general anesthesia, and dicaine hydrochloride eye drops were used for local anesthesia. Intraocular pressure was first reduced by a puncture at the edge of the cornea. A 33G microinjector needle on a 5  $\mu\text{L}$  syringe (Hamilton) was inserted into the temporal side of the eye through the cornea, conjunctiva, and sclera, finally reaching the subretinal space, and forming a self-sealing wound. About 1  $\mu\text{L}$  of cell suspension ( $2\times 10^4$  cells/ $\mu\text{L}$ ), or 1  $\mu\text{L}$  of SHEDs-CM, and balanced medium containing sodium fluorescein, but not serum, was injected into the subretinal space. Successful injection was confirmed by the presence of yellow-green fluorescent liquid in the fundus. Levofloxacin hydrochloride eye drops (Zhuhai United Laboratories) were applied topically to the eye three times/day for 3 days after injection.

### Electroretinogram

To assess the recovery of visual function, electroretinogram (ERG) was recorded in mice at 1, 2, and 4 months ( $n=6-8$  eyes/group at each time point) after subretinal treatment using a RETI system with RETIport Science 4.8.5.0 software (Roland Consult). The visual evoked potential and the International Society for Clinical Electrophysiology of Vision ERG Ganzfeld (ISCEV-ERG GF) program were used to record standard ERGs. Mice were dark adapted overnight before ERG recording. Under dim red light, mice were anaesthetized by injection of 4% chloral hydrate (400 mg/kg i.p.) and the pupils were dilated with tropicamide, xylazine (10 mg/kg), and ketamine (100 mg/kg). Hydroxypropyl methylcellulose was applied regularly to the cornea to prevent dehydration and allow for optimal electrical conductivity. Each mouse was positioned on a heating pad with a ground electrode inserted into the tail and a reference electrode subcutaneously in the cheek. The positions of the corneal electrodes were adjusted for the best light stimulation and electrode contact. Each eye was first stimulated at a light intensity of  $0.01\text{ cd}\cdot\text{s}/\text{m}^2$ , and then the animals were light adapted for 10 min before stimulation at a light intensity of  $3.0\text{ cd}\cdot\text{s}/\text{m}^2$ . ERG waves were recorded six times for each response at interstimulus intervals of 1 s, and the average wave was saved for further analysis.

### Histological analysis

The mice were sacrificed after the ERG test under general anesthesia and the eyes were removed ( $n=6-8$  eyes/group at each time point) and immersed in 4% paraformaldehyde (PFA) for 4 h. Then, they were infiltrated with 20% sucrose

for at least 24 h and 30% for  $\sim 12$  h until they sank, and next they were embedded in O.C.T. Compound (Sakura) with the vertical meridian of the eye through both the optic nerve and the injection site and in the cutting orientation. Sections were cut at 5  $\mu\text{m}$  and stored at  $-20^\circ\text{C}$ . We obtained 50–80 sections from each eye, and areas 500–1,500  $\mu\text{m}$  from the optic nerve head containing the injection site were observed under microscopes (confocal; Zeiss or fluorescence; Olympus).

Hematoxylin and eosin staining was performed to show retinal structure, especially ONL photoreceptors. Cell layers from three locations in the injection site were counted in every section, and the average counts were recorded.

Immunofluorescence was performed to observe the outer segment (OS) of the photoreceptor. In brief, sections were fixed in 4% PFA at room temperature for 10 min, and then gently rinsed three times with PBS, 5 min each time. Then the sections were immersed in 1% bovine serum albumin containing 0.1% Triton X-100 for 30 min at  $37^\circ\text{C}$ , and incubated overnight with primary antibodies (Supplementary Table S5) at  $4^\circ\text{C}$ . The sections were gently rinsed three times with PBS, 10 min each time, then incubated in the dark with the secondary antibodies Alexa Fluor 594-conjugated AffiniPure goat anti-rabbit immunoglobulin G (IgG) (H + L) (Proteintech) and Alexa Fluor 488 or 594-conjugated AffiniPure goat anti-mouse IgG (H + L) (Proteintech) for 1 h at  $37^\circ\text{C}$ . After rinsing, the sections were finally counterstained with 4', 6-diamidino-2-phenylindole (DAPI), and viewed under a fluorescence microscope (Olympus) or a laser-scanning confocal microscope (Zeiss). In each immunofluorescence experiment, we set up negative controls in which the primary antibody was not used.

### TUNEL staining

TUNEL staining was performed using an In Situ Cell Death Detection Kit, Fluorescein (Roche), according to the manufacturer's instructions. In brief, cryopreserved sections were fixed with 4% PFA at room temperature for 10 min, and then gently rinsed three times with PBS, 5 min each time. The sections were then treated with the freshly prepared permeabilization solution 0.1% Triton X-100 in 0.1% sodium citrate at  $4^\circ\text{C}$  for 10 min. Then, they were incubated with the TUNEL reaction mixture (Enzyme Solution:Label Solution, 1:9) at  $37^\circ\text{C}$  for 60 min in a humidified atmosphere in the dark, and counterstained with DAPI. Finally, the sections were viewed under a laser-scanning confocal microscope (Zeiss), and the relative intensity was quantified using the ZEN (Blue) software (Zeiss).

### Senescence $\beta$ -galactosidase staining

Galactosidase staining was performed using a senescence  $\beta$ -galactosidase staining kit (Beyotime, China) according to the manufacturer's instructions. In brief, SHEDs or retinal-induced SHEDs on day 24 were fixed with 4% PFA for 15 min at room temperature, and then washed three times with PBS. The cells were incubated with the staining working solution at  $37^\circ\text{C}$  in a humidified atmosphere, washed again, and observed under an inverted phase-contrast microscope (Olympus).

### Statistical analysis

All experiments included at least three biological replicates and experimental replicates. Quantitative reverse transcription-polymerase chain reaction data were compared using two-tailed *t*-tests for independent samples. The maximum b-wave in ERG, number of cell layers in the ONL, and TUNEL intensity were analyzed using one-way analysis of variance in GraphPad Prism 7 (La Jolla). Statistical significance was set at  $P < 0.05$ . Data are shown as the mean  $\pm$  standard deviation.

### Results

#### Optimal induction time of SHEDs for transplantation

To improve the survival and compatibility of SHEDs in vivo, the best induction time of SHEDs for transplanta-

tion has to be determined first. By using the two-step induction procedure, we found that the gene expression of the retinal precursor biomarkers (*RCVRN*, *NRL*, and *AIPL1*) started increasing after 14 days, and mature photoreceptor biomarkers (*RHO* and *OPN1SW*) maintained low levels of expression until 24 days (Fig. 1A). *GLUL* and *STXBPI*, representing neuronal activity, were upregulated at 14 days (Fig. 1B). Genes representing  $Ca^{2+}$  channel activity (*SSH1*, *ITPR2*, and *CAMK2D*), which have neuronal characteristics, showed an increasing trend or peaks in expression at  $\sim 14$  days (Fig. 1C); and the biomarkers of antioxidation activity (*SOD2*, *TXNRD2*, and *SOD1*), which favor the survival of transplanted cells, showed a similar trend (Fig. 1D). SHEDs induced at  $\sim 14$  days may be in the appropriate state for the genesis of retinal neuron progenitors.

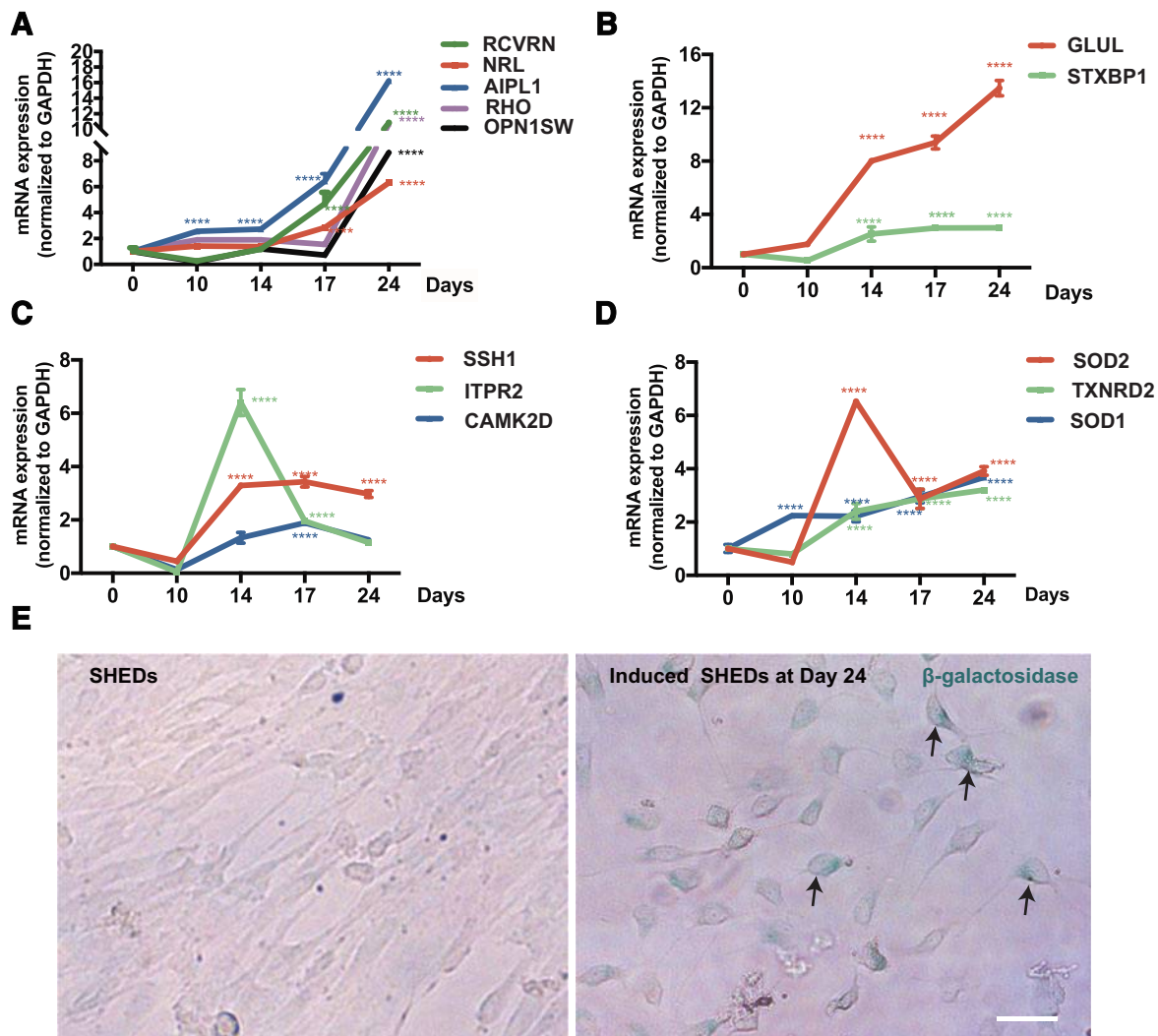


**FIG. 1.** Optimal induction time of SHEDs for transplantation is  $\sim 14$  days. (A–D) Quantitative polymerase chain reaction analysis showing that the relative gene expression of retinal precursor biomarkers (*RCVRN*, *NRL* and *AIPL1*) is upregulated since day 10, and mature photoreceptor biomarkers (*RHO* and *OPN1SW*) maintained low levels of expression until day 17 (A). Genes representing neuron activity (*GLUL* and *STXBPI*) were upregulated since day 14 (B). Biomarkers of calcium channel activity (*SSH1*, *ITPR2*, and *CAMK2D*), and antioxidation activity (*SOD2*, *TXNRD2*, and *SOD1*) showed an increasing trend or at peaks in expression at  $\sim 14$  days (C, D) ( $***P < 0.001$  and  $****P < 0.0001$ ) (E). Microscope images showing noninduced SHEDs are negative for  $\beta$ -galactosidase staining, as indicated by green–blue accumulation in the cells (black arrows), while induced SHEDs on day 24 are positive for  $\beta$ -galactosidase staining. Scale bar: 50  $\mu$ m. SHED, stem cell from exfoliated deciduous teeth. Color images are available online.

Furthermore, our pilot study showed that noninduced SHEDs were seldom found in the subretinal space 1 month after transplantation, while induced SHEDs survived better and were detected even 4 months after injection (Supplementary Fig. S1).  $\beta$ -Galactosidase staining indicated that terminally differentiated SHEDs on day 24 were positive for  $\beta$ -galactosidase staining and showed signs of senescence (Fig. 1E). Above all, we concluded that SHEDs induced at  $\sim$ 14 days would be optimal for transplantation, and they were used in the following experiments.

### *SHEDs and SHEDs-CM enhanced dark-adapted and light-adapted ERG responses*

ERG testing enables the direct assessment of photoreceptors (a-wave component) and second-order neurons (b-wave component). Dark-adapted 0.01 ERG is used to assess the function of rods and their second-order bipolar cells, and light-adapted 3.0 ERG is used to assess the function of cones and their second-order neurons. The b wave was measured as the value from the trough to the peak for comparison. In dark-adapted 0.01 ERG, the b wave amplitude was much higher in SHED- and SHEDs-CM-treated eyes than that in the control eyes at 1 month ( $P < 0.01$ ) and 2 months ( $P < 0.05$ ) after treatment (Fig. 2A), but the difference among the three groups disappeared at 4 months. At every time point, there was no statistical difference between SHED- and SHEDs-CM-treated eyes. All groups showed a descending trend of b-waves with time, and some control eyes showed flat or even unmeasurable ERG responses after surgery. Representative ERGs showed that b-wave amplitudes were much higher in SHED- and SHEDs-CM-treated eyes than that in the control eyes at 1 and 2 months after treatment (Fig. 2B, C), and were almost the same among the three groups 2 months after treatment (Fig. 2D).

In light-adapted 3.0 ERG, b-wave amplitudes were much higher in SHED- and SHEDs-CM-treated eyes than that in the control eyes at 1 month ( $P < 0.01$ ), 2 months ( $P < 0.05$ ), and 4 months ( $P < 0.05$ ) after treatment (Fig. 2E). At every time point, there was no statistical difference between SHED- and SHEDs-CM-treated eyes. All groups showed a descending trend of b-waves with time, and some control eyes showed flat or even unmeasurable ERG responses at 4 months after surgery. Representative ERGs showed that b-wave amplitudes were much higher in SHED- and SHEDs-CM-treated eyes than that in the control eyes 1, 2, and 4 months after treatment (Fig. 2F–H).

### *SHED and SHEDs-CM treatment ameliorated photoreceptor degeneration*

To determine whether photoreceptors survived better after treatment with SHEDs and SHEDs-CM, we counted the number of cells in the ONL. In accordance with the rescue of visual function, histological analysis of the retinas at different time points following SHED and SHEDs-CM treatment revealed extensive photoreceptor rescue across most of the retina 1 month (Fig. 3A–C), 2 months (Fig. 3D–F), and 4 months (Fig. 3G–I) after treatment. The cell numbers in the ONL in SHED- and SHEDs-CM-treated retinas were higher than those of control retinas at all three time points (Fig. 3J–L). At 1 month after treatment, the

number of cell layers in the ONL were  $8.9 \pm 0.6$  (control),  $10.1 \pm 1.4$  (SHEDs), and  $10.3 \pm 1.0$  (SHED-CM); at 2 months, the values were  $8.5 \pm 0.6$ ,  $10.0 \pm 1.3$ , and  $9.7 \pm 0.8$ ; and at 4 months, they were  $8.2 \pm 0.7$ ,  $9.1 \pm 0.6$ , and  $9.4 \pm 0.9$ . There was no statistical difference between the SHED- and SHEDs-CM-treated retinas at any time point.

### *SHEDs and SHEDs-CM maintained the structure of the OSs of photoreceptors*

Rhodopsin is the biomarker of rods and opsin is the biomarker of cones. Immunoreactivity against rhodopsin and opsin showed that the degeneration of rods and cones were attenuated by treatment with SHEDs and SHEDs-CM, and this was in accord with the rescue of visual function. At 1 month after treatment, rhodopsin in the OS of the control retinas became disorganized and loose (Fig. 4A1), while in the treated retinas, the OS remained well organized and tightly arranged (Fig. 4A2, A3). At 2 months, the expression of rhodopsin decreased markedly and the OS became much thinner in the control retinas (Fig. 4A4), while rhodopsin remained and the OS was well organized in treated retinas (Fig. 4A5, A6). At 4 months, rhodopsin decomposed further in the control retinas than that in the treated retinas (Fig. 4A7–A9). Retinas treated with SHEDs and SHEDs-CM showed signs of decomposition at 4 months after treatment (Fig. 4A8, A9).

In the control retinas, at 1 month, the opsin in the OS was partly decomposed (Fig. 4B1), at 2 months, it decomposed further (Fig. 4B4), and at 4 months, it was rarely found (Fig. 4B7). In the treated retinas at 1 month, the OS remained well organized and tightly arranged (Fig. 4B2, B3), at 2 months, it remained relatively well organized, although less dense (Fig. 4B5, B6), and at 4 months, the OS showed signs of disorganization (Fig. 4B8, B9).

### *SHEDs and SHEDs-CM exerted antiapoptotic activity*

It has been reported that apoptosis [24] and reactive gliosis [25] are pathological changes in mice with RP. At 4 months, there were more TUNEL-stained cells in the ONL of control retinas than those treated with SHEDs or SHEDs-CM (Fig. 5A). The relative density of apoptotic cells in the ONL for each microscope field was  $18.6 \pm 1.1$  in the control group,  $11.4 \pm 1.4$  in the SHED group, and  $11.1 \pm 1.4$  in the SHEDs-CM group; there were no significant differences between the latter two groups (Fig. 5).

## **Discussion**

The reparative effects of MSCs in restoring retinal function include two mechanisms: one is cell replacement, based on neural differentiation, and the other is their paracrine actions that have favorable effects such as neurotrophic protection, immunomodulation, antiapoptosis, anti-inflammation, and regulation of angiogenesis [26]. In this study, we used induced SHEDs and collected SHEDs-CM to test for their possible therapeutic effects on retinal degeneration. The results demonstrated that both SHED and SHEDs-CM treatment enhanced the dark-adapted and light-adapted ERG responses, ameliorated photoreceptor degeneration, maintained the structure of the OS of photoreceptors, and had an

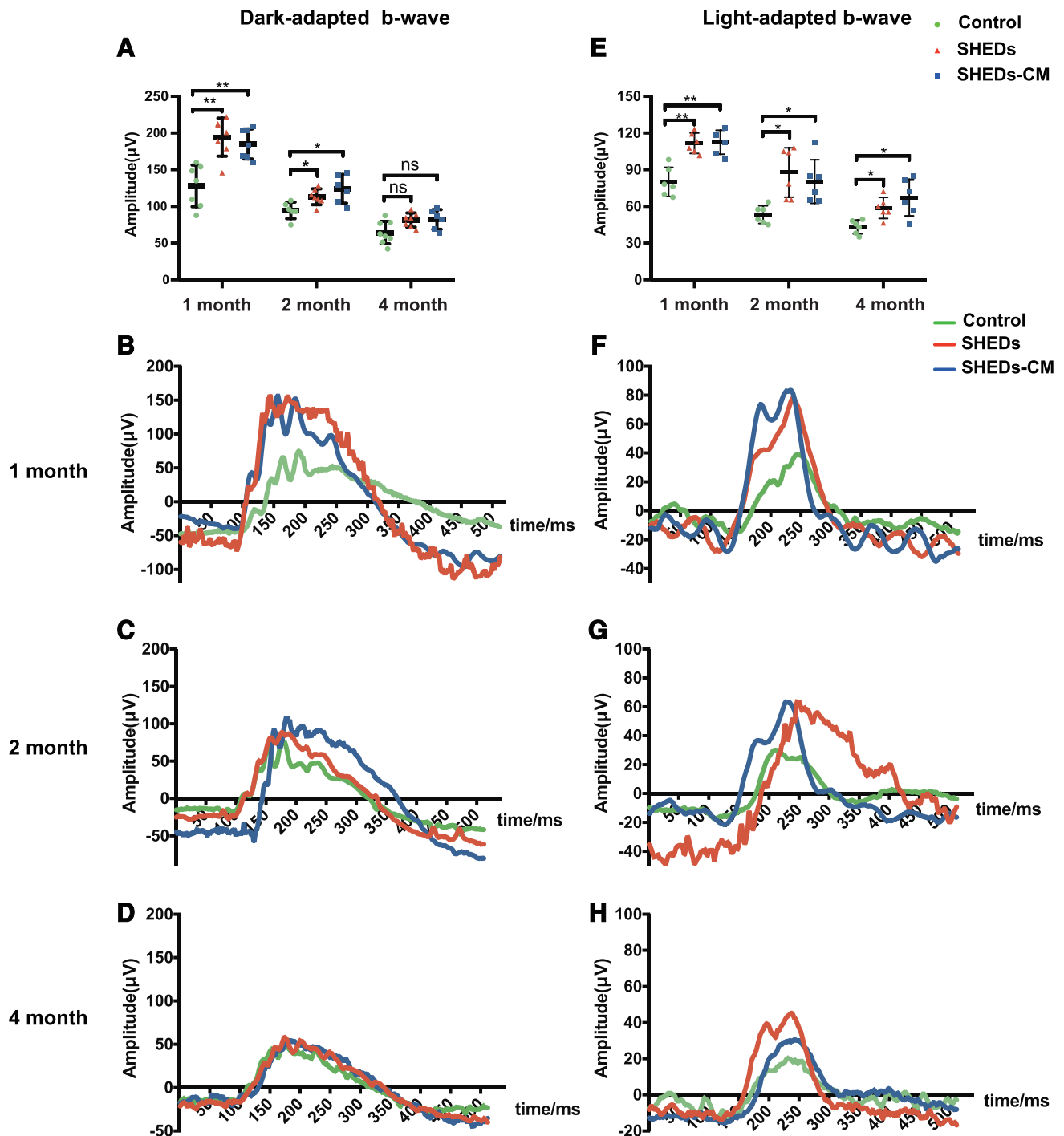


**FIG. 2.** Treatment with SHEDs and SHEDs-CM enhanced dark-adapted and light-adapted ERG responses. Analysis of dark-adapted 0.01 ERG showing the maximum b-wave amplitudes of control, SHED, and SHEDs-CM group in 1, 2, and 4 months after treatment (**A**). Representative dark-adapted 0.01 ERG of control, SHED, and SHEDs-CM group in 1 (**B**), 2 (**C**), and 4 (**D**) months after treatment. Analysis of light-adapted 3.0 ERG showing the maximum b-wave amplitudes of control, SHED, and SHEDs-CM group in 1, 2, and 4 months after treatment (**E**). Representative light-adapted 3.0 ERG of control, SHED, and SHEDs-CM group in 1 (**F**), 2 (**G**), and 4 (**H**) months after treatment. (\* $P < 0.05$  and \*\* $P < 0.01$ ). ERG, electroretinogram; ns, not statistically significant ( $P > 0.05$ ). SHEDs-CM, conditioned medium derived from SHEDs. Color images are available online.

antiapoptotic effect. Induced SHEDs did not replace the injured photoreceptors directly, neither did they differentiate further in vivo nor integrate into the host retina (Fig. 6). Over time, the therapeutic effects weakened. The results are consistent with other studies that demonstrated MSCs more commonly have neurotrophic and neuroprotective effects on

photoreceptor rather than replacing cells [27–30]. No tumor formation or worsening physical condition was observed in the mice. Since a limited number of mice were used in this study, a longer follow-up is needed to define safety measures and to identify factors influencing the extent and duration of visual recovery.

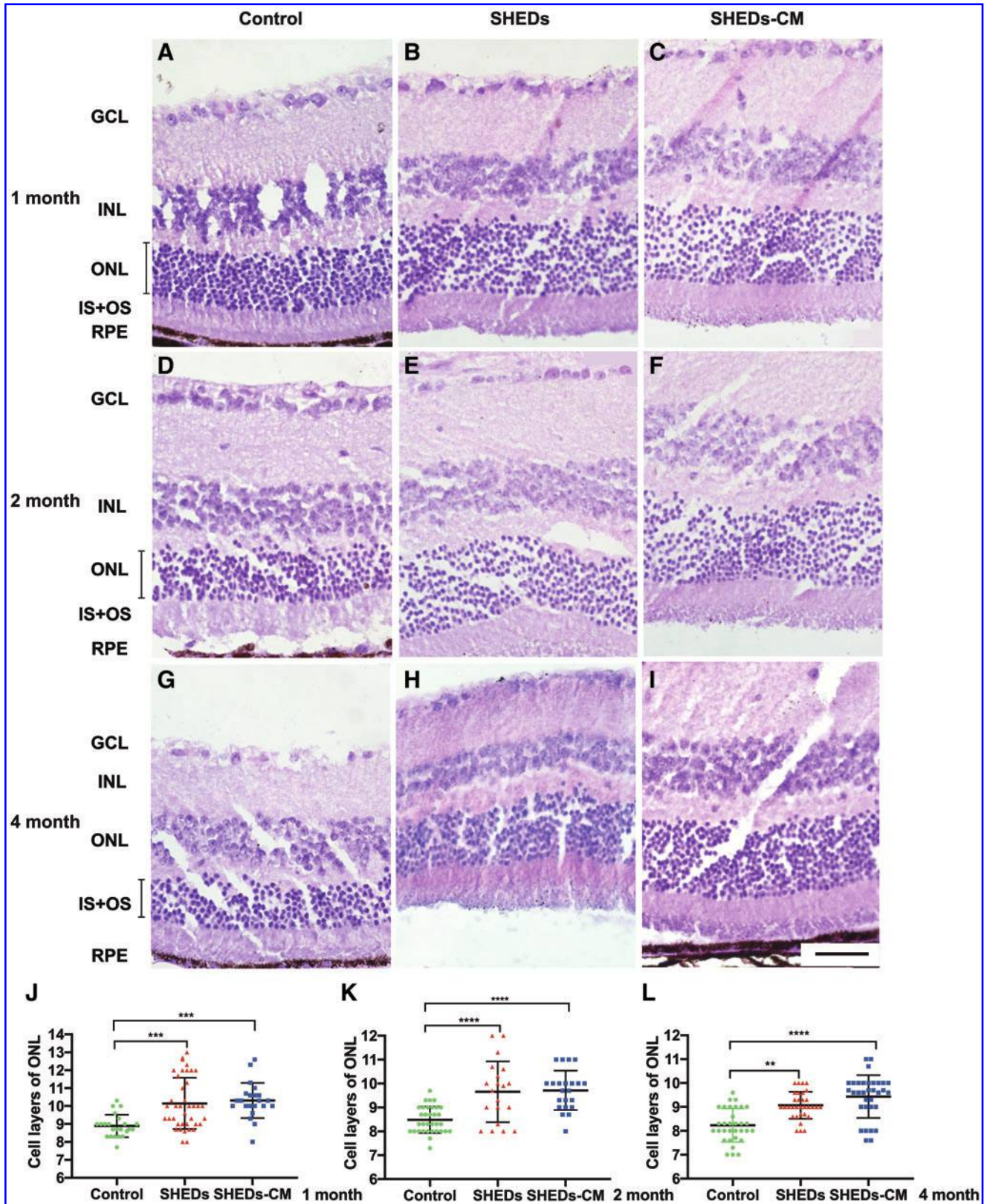


**FIG. 3.** Photoreceptors were rescued following subretinal injection of SHEDs and SHEDs-CM. Hematoxylin and eosin-stained sections at 1 month (A–C), 2 months (D–F), and 4 months (G–I) in control-, SHED-, SHEDs-CM-treated eyes. *Black lines* emphasize ONL length. Scale bar: 50  $\mu$ m. Plots showing the number of cell layers in the ONL at 1 month (J), 2 months (K), and 4 months (L) after treatment. Scale bar: 40  $\mu$ m. (\*\* $P$  < 0.01, \*\*\* $P$  < 0.001, and \*\*\*\* $P$  < 0.0001). INL, inner nuclear layer; ONL, outer nuclear layer; RPE, retinal epithelial cells; IS, inner segment; OS, outer segment; GCL, ganglion cell layer. Color images are available online.

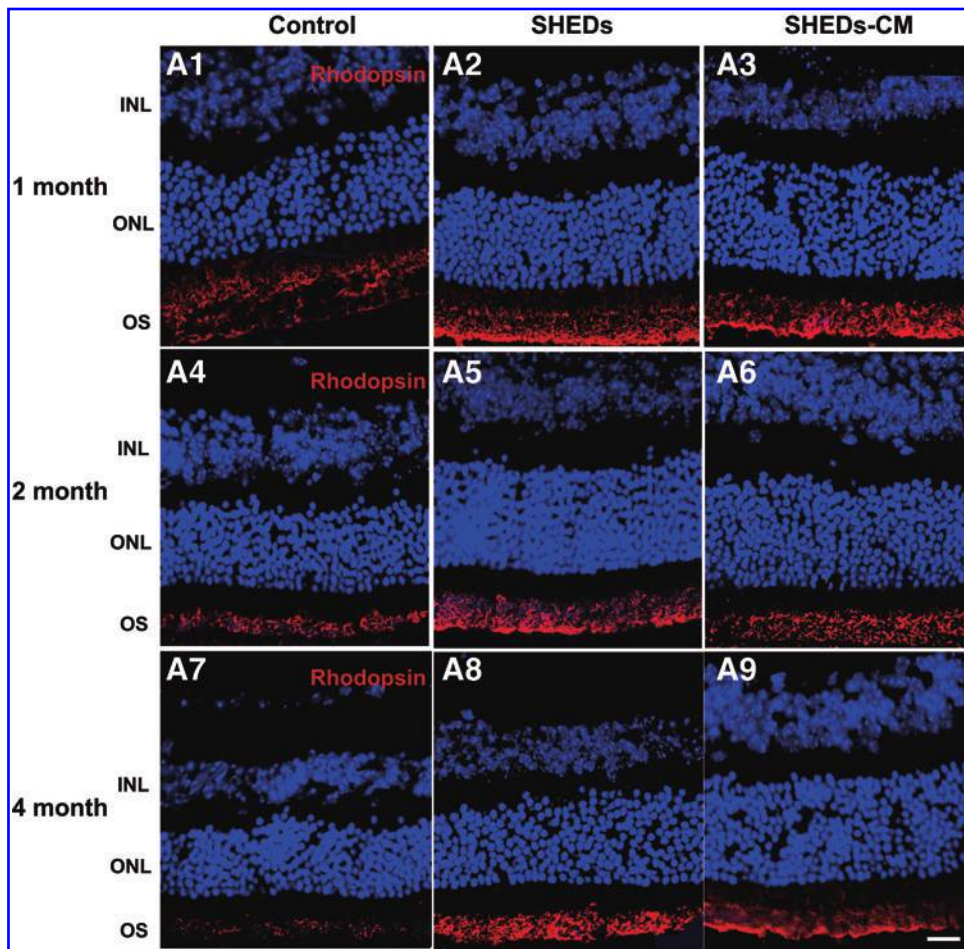


**FIG. 4.** Treatment with SHEDs and SHEDs-CM preserved the structure of rods and cones. (A1–A9) Rhodopsin staining (red) and DAPI counterstaining of retinas at 1 month (A1–A3), 2 months (A4–A6), and 4 months (A7–A9) after treatment in control, SHED, and SHEDs-CM group. (B1–B9) Opsin staining (red) and DAPI counterstaining of retinas at 1 month (B1–B3), 2 months (B4–B6), and 4 months (B7–B9) after treatment in control, SHED, and SHEDs-CM group. Scale bars: 20  $\mu\text{m}$ . DAPI, 4',6'-diamidino-2-phenylindole. Color images are available online.

(continued)

In this study, we found that the most suitable induction time of SHEDs for transplantation is  $\sim 14$  days, a time coincident with the genesis of retinal neuron progenitors. It has been reported that terminally differentiated cells are not suitable for transplantation, as they are too mature and lack the ability to incorporate into the host tissues or further differentiate into photoreceptors [11]; we found indications of senescence in retinal-induced SHEDs on day 24. A previous study reported that neuronal-induced SHEDs are more effective in promoting neuronal and glial differentiation in a rat model of spinal cord injury than undifferentiated SHEDs [19]; and in this study, noninduced SHEDs did not survive as well as induced SHEDs. In addition, our previous study showed that differentiated SHEDs on days 14–17 begin to show a neuron-like morphology of cells and are sustainable *in vivo* 3 months after transplantation in mice [23], and in this study, they showed a trend of upregulation of the expression of genes associated with neurons and antioxidantation. Thus, we used SHEDs induced for  $\sim 14$  days for transplantation.

Subretinal injection allows SHEDs or SHEDs-CM to contact the photoreceptors directly. One microliter of solution injected into the subretinal space usually did not detach the ONL from the retinal pigment epithelium. In our study, four mice (from all three groups) showed signs of surgical damage and no ERG responses, and we removed these mice from the study. The mice did not show any signs of reactive gliosis (Supplementary Fig. S2). This differs from a previous study demonstrating that gliosis is initiated in 2-month-

old mice with RP [25]. This may be because the molecular mechanisms and hereditary rhodopsin mutants of RP are complex and various; different knockout mouse models of RP may have different pathologies [31,32]. And the mice used in this study did not reach the point when gliosis was initiated. Above all, subretinal space transplantation is a mature and widely used method.

We used  $\sim 4$ -month-old mice. One study has reported that it is possible the efficacy is improved if treatment is given before visual impairment and retinal degeneration are established, such as in a pediatric population [33]. Another study has demonstrated that delayed treatment may lead to the photoreceptors becoming locked in a metabolically abnormal proapoptotic state, making them refractory to treatment [24]. At 4 months of age in mice, the retinal degeneration has started, but has yet to reach the peak of degeneration, so this is a suitable time for stem cell treatment.

The duration and outcome of transplanted stem cells *in vivo* have been explored for a long time. We have confirmed that SHEDs have the potential to differentiate into photoreceptor-like cells *in vitro*, and they survived well for at least 21 days in the subretinal space as shown by *in vivo* bioluminescence imaging, and were detectable for 3 months, as previously reported [23]. However, there was no evidence of further cell differentiation or replacement *in vivo*, even though SHEDs were retina induced for  $\sim 14$  days *in vitro* before use. In this study, only sparse SHEDs were detected in the subretinal space at 4 months after transplantation, and

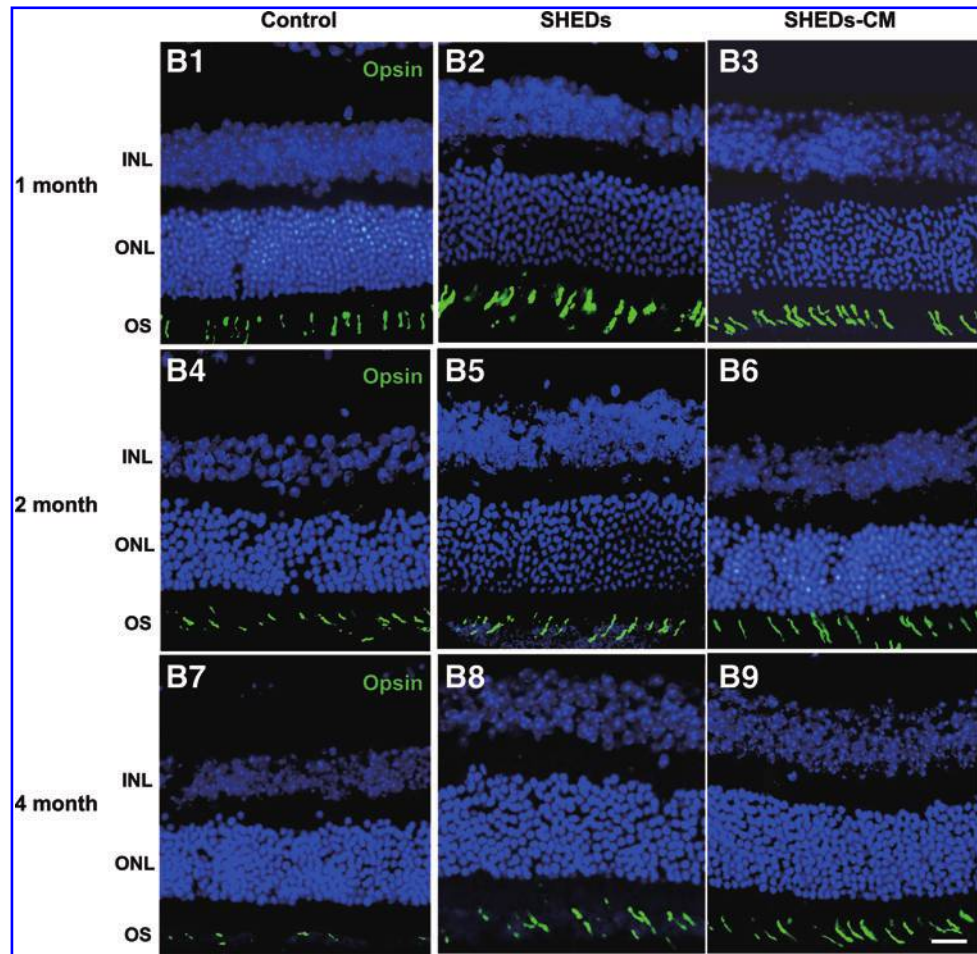


FIG. 4. (Continued).

none was detected in the ONL or inner nuclear layer (INL). It seems that most transplanted exogenous MSCs survived for only a short time. This may be related to the immune microenvironment. An intact eye is generally considered to be an immune-privileged site that protects engrafted exogenous tissues from uncontrolled immune rejection. The eye supports grafted tissue or cells for extended or indefinite periods of time without rejection [34,35]. However, in cases of injury, damage, or degeneration of the eye, this protection is compromised and immune cell infiltration necessary for repair occurs [36,37]. Despite the immunomodulatory activity of MSCs, there still seem to be problems of immunorejection and compromised immunomodulation when it comes to cross-species transplantation. It has recently been reported that human xenografts of MSCs do not prolong corneal allograft survival in rats and fail to suppress rat T cell proliferation due to interspecies incompatibility in cytokine signaling [38]. However, the allogeneic transplanted MSCs do prolong corneal allograft survival by suppressing peripheral immune responses and promoting the host immunomodulatory niche [39]. Another factor may be that exogenously transplanted SHEDs themselves cannot adapt to the host retinal niche to survive in the long term. Therefore, it is reasonable to conclude that most human SHEDs are finally removed from the subretinal space. Interspecies incompatibilities should be taken into consider-

ation when analogizing preclinical false-negative data to clinical trials. Although transplanted SHEDs decreased markedly with time in vivo in this study, we anticipate better survival of transplanted SHEDs when applied in an autologous or allogeneic manner.

It seems that transplanted cells do not have to persist in vivo to achieve therapeutic effects. In this study, 21 days of good survival of SHEDs indicated by in vivo bioluminescence imaging [23] brought 4 months of retinal structural and functional improvement. Similarly, 2 weeks of cell survival results in improved retinal function for up to 20 weeks following transplantation [29], and 6 weeks of cell survival rescues retinal function up to 20 weeks [28]. The reason why therapeutic effects last longer than cell persistence in vivo is unclear now.

SHEDs themselves did not replace injured photoreceptors, and we infer that the therapeutic effects are mainly mediated by paracrine secreta. In this study, the SHEDs-CM group further confirmed this point. SHEDs-CM had almost the same therapeutic effects as SHEDs. Conditioned medium from MSCs has been considered a safe and effective alternative to stem cell therapy without the risk of immune rejection and tumorigenesis. SHEDs-CM contains cytokines, growth factors, extracellular vesicles (including exosomes and microvesicles), and other components that have therapeutic effects. We hypothesize that both SHEDs and SHEDs-CM

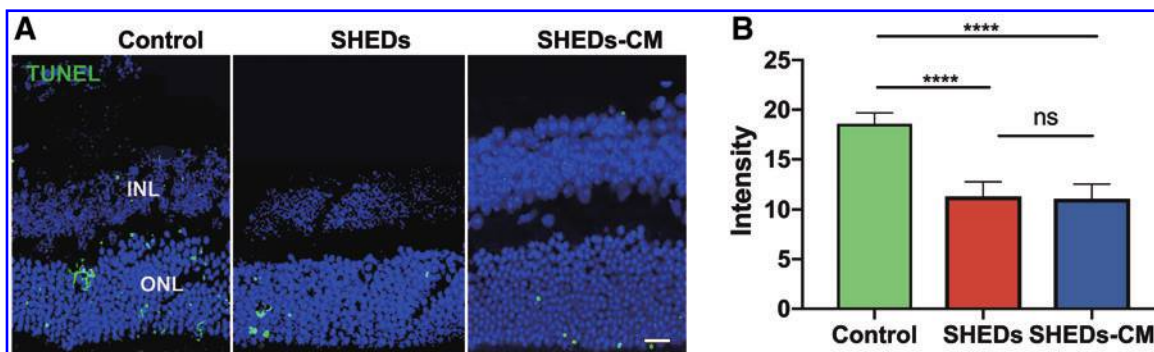


**FIG. 5.** SHEDs exerted antiapoptotic activity. TUNEL staining showing the dyed nucleus in the ONL in control, SHED, and SHEDs-CM group at 4 months after treatment (A). Control retinas have larger amount of apoptotic nuclei in the ONL than SHED or SHEDs-CM group (B) at 4 months after treatment (\*\*\*\* $P < 0.0001$ ). Scale bar: 20  $\mu\text{m}$ . Color images are available online.

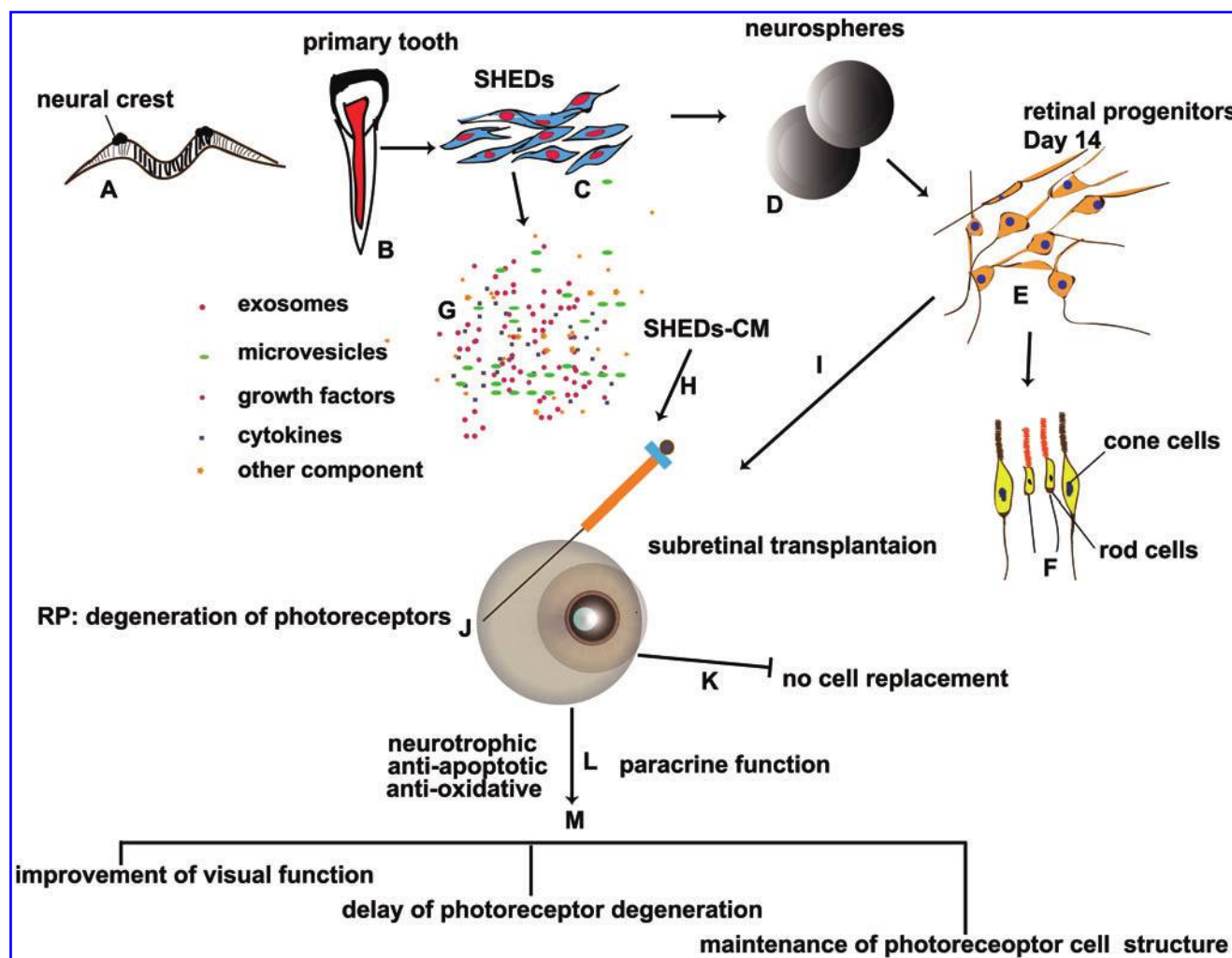


**FIG. 6.** The scheme demonstrates the design and results of this study. (A, B) Primary teeth originate from neural crest in embryonic development. (B, C) Stem cells are isolated from the pulp of the primary teeth, and named as SHEDs. (D–F) SHEDs have the potential to differentiate toward retinal photoreceptor-like cells in vitro under certain induction. SHEDs form neurosphere-like cell masses after floating culture (D), then differentiate toward photoreceptors in adherent culture (F), and generate retinal progenitor-like cells on day 14 (E). (G) SHEDs secrete rich components including growth factors, cytokines, exosomes, microvesicles, and other components, which exert paracrine function. (H–J) Induced SHEDs on day 14 and ultrafiltrated SHEDs-CM are used for subretinal transplantation in RP eyes. (K) There is no sign of cell replacement after cell transplantation. (L) Both SHEDs-CM and SHEDs exert paracrine function such as neurotrophic, antiapoptotic, and the potential antioxidative activity. (M) Therapeutic effects include restoration of visual function, amelioration of photoreceptor degeneration, and maintenance of normal structure of photoreceptors. RP, retinitis pigmentosa. Color images are available online.

exert effects by stimulating host tissues toward self-protection and self-repair, not just direct neuroprotection. The mechanisms by how the SHEDs-CM have an effect that lasts months remain to be clarified by further research.

Many researchers pointed out that MSCs exert effects mainly through paracrine/endocrine function, not cell replacement, and agree with a concept of cell-free therapy [28,40–42]. Thus, it is reasonable that SHEDs and SHEDs-CM show the same therapeutic effects. Regarding different mechanisms of therapeutic effects between cells and their CM, there are seldom studies that particularly address this problem. Recently, components of MSC-conditioned medium that are effective in treating retinal diseases have been further studied. Intravitreal administration of exosomes derived from human MSCs is well tolerated without immunosuppression and decreases the severity of retinal ischemia in mouse models [43]. Exosomes derived from umbilical cord MSCs integrate into both neurons and astrocytes of the inner retina 24 h after vitreous injection [40]. However, it is very interesting that similar studies on using MSCs and their CM to treat kidney injury showed different results. One study reports that MSCs and their CM were both potent in ameliorating cisplatin-induced kidney failure [44]. Another study reports that CM did not improve retinal function as the MSCs did, and even consecutive and high-dose injections of CM (regarding the short half-life of CM components) did not show better therapeutic effects [45]. MSCs' secretome can be modulated by preconditioning the MSCs during *in vitro* culture [46,47]. It seems the ways of preparing CM and the methods of giving cells and CM into animals, as well as animal models of different pathology influence the therapeutic effects of CM.

CM composes complex components whose detailed function in treating diseases is yet to be clarified. In this study, we used concentrated SHEDs-CM, not a single component such as exosomes. It is demonstrated that exosomes from different MSC types are different, and are responsible for a specific therapeutic effect [48]. The components in SHEDs-CM, and their cargos (proteins, mRNAs, and lipids) may influence their effects on host tissues. One study reports that exosomes rather than microvesicles protect retinal ganglion cells, which is mediated by their miRNA rather than protein content [41]. Another study showed that microvesicles inhibit neurogenesis, while exosomes augment it [49]. It is demonstrated that exosomes play a role in immunomodulation and immune privilege of the eye [50]. The eventual effects of SHEDs-CM *in vivo* remain unknown, and a feasible way to label its components first needs to be developed for *in vivo* tracking. The structure of the INL, mainly composed of bipolar cells, was well preserved in the control and SHED- and SHEDs-CM-treated groups (Supplementary Fig. S3), so it is not clear whether components in the SHEDs-CM or secreted by SHEDs reached the INL.

The mechanisms how SHEDs and SHEDs-CM improve retinal structure and function need to be further explored. And the possible difference of paracrine function between induced SHEDs and noninduced SHEDs remains blankly unknown.

SHEDs, which originate from the neural crest, are easy to harvest and establish a stem cell bank, safe to use, and have no ethical consequences, are becoming an attractive source for cell-based or cell-free therapy to treat retinal degeneration, including RP.

## Conclusion

In conclusion, our results provide evidence that both SHEDs and SHEDs-CM have therapeutic effects by enhancing visual function, delaying the degeneration of photoreceptors, and maintaining the structure of OSs of photoreceptors in a mouse model of retinal degeneration. They both showed antiapoptotic activity. Thus, SHEDs are a promising stem cell source for restoring vision in patients with degenerative retinal diseases.

## Author Disclosure Statement

No competing financial interests exist.

## Funding Information

This study was supported by grants from the National Natural Science Foundation of China (303076129, 81772873, 81970920), Beijing Natural Science Foundation (7172240, 7182181), and the Stomatology Development Fund of Tason.

## Supplementary Material

Supplementary Figure S1  
Supplementary Figure S2  
Supplementary Figure S3  
Supplementary Table S1  
Supplementary Table S2  
Supplementary Table S3  
Supplementary Table S4  
Supplementary Table S5

## References

- Hartong DT, EL Berson and TP Dryja. (2006). Retinitis pigmentosa. *Lancet* 368:1795–1809.
- Milam AH, ZY Li and RN Fariss. (1998). Histopathology of the human retina in retinitis pigmentosa. *Prog Retin Eye Res* 17:175–205.
- Grover S, GA Fishman, RJ Anderson, MSV Tozatti, JR Heckenlively, RG Weleber, AO Edwards and J Brown. (1999). Visual acuity impairment in patients with retinitis pigmentosa at age 45 years or older. *Ophthalmology* 106:1780–1785.
- Ho AC, MS Humayun, JD Dorn, L da Cruz, G Dagnelie, J Handa, P-O Barale, J-A Sahel, PE Stanga, et al. (2015). Long-term results from an epiretinal prosthesis to restore sight to the blind. *Ophthalmology* 122:1547–1554.
- Russell S, J Bennett, JA Wellman, DC Chung, Z-F Yu, A Tillman, J Wittes, J Pappas, O Elci, et al. (2017). Efficacy and safety of voretigene neparvovec (AAV2-hRPE65v2) in patients with RPE65-mediated inherited retinal dystrophy: a randomised, controlled, open-label, phase 3 trial. *Lancet* 390:849–860.
- Miraldi Utz V, RG Coussa, F Antaki and EI Traboulsi. (2018). Gene therapy for RPE65-related retinal disease. *Ophthalmic Genet* 39:671–677.
- Klassen H. (2016). Stem cells in clinical trials for treatment of retinal degeneration. *Expert Opin Biol Ther* 16:7–14.
- Kaplan HJ, TH Tezel, AS Berger, ML Wolf and LV DelPriore. (1997). Human photoreceptor transplantation in retinitis pigmentosa—a safety study. *Arch Ophthalmol* 115:1168–1172.
- Das T, M del Cerro, S Jalali, VS Rao, VK Gullapalli, C Little, DA Loreto, S Sharma, A Sreedharan, C del Cerro and GN Rao. (1999). The transplantation of human fetal

- neuroretinal cells in advanced retinitis pigmentosa patients: results of a long-term safety study. *Exp Neurol* 157:58–68.
10. Radtke ND, RB Aramant, M Seiler and HM Petry. (1999). Preliminary report: indications of improved visual function after retinal sheet transplantation in retinitis pigmentosa patients. *Am J Ophthalmol* 128:384–387.
  11. MacLaren RE, RA Pearson, A MacNeil, RH Douglas, TE Salt, M Akimoto, A Swaroop, JC Sowden and RR Ali. (2006). Retinal repair by transplantation of photoreceptor precursors. *Nature* 444:203–207.
  12. Assawachananont J, M Mandai, S Okamoto, C Yamada, M Eiraku, S Yonemura, Y Sasai and M Takahashi. (2014). Transplantation of embryonic and induced pluripotent stem cell-derived 3D retinal sheets into retinal degenerative mice. *Stem Cell Rep* 2:662–674.
  13. Gonzalez-Cordero A, K Kruczek, A Naeem, M Fernando, M Kloc, J Ribeiro, D Goh, Y Duran, SJI Blackford, et al. (2017). Recapitulation of human retinal development from human pluripotent stem cells generates transplantable populations of cone photoreceptors. *Stem Cell Rep* 9:820–837.
  14. Mandai M, M Fujii, T Hashiguchi, GA Sunagawa, SI Ito, J Sun, J Kaneko, J Sho, C Yamada and M Takahashi. (2017). iPSC-derived retina transplants improve vision in rd1 end-stage retinal-degeneration mice. *Stem Cell Rep* 8:1112–1113.
  15. Miura M, S Gronthos, M Zhao, B Lu, LW Fisher, PG Robey and S Shi. (2003). SHED: stem cells from human exfoliated deciduous teeth. *Proc Natl Acad Sci U S A* 100:5807–5812.
  16. Kerkis I, A Kerkis, D Dozortsev, GC Stukart-Parsons, SM Gomes Massironi, LV Pereira, AI Caplan and HF Cerruti. (2006). Isolation and characterization of a population of immature dental pulp stem cells expressing OCT-4 and other embryonic stem cell markers. *Cells Tissues Organs* 184:105–116.
  17. Yamaza T, A Kentaro, C Chen, Y Liu, Y Shi, S Gronthos, S Wang and S Shi. (2010). Immunomodulatory properties of stem cells from exfoliated deciduous teeth. *Stem Cell Res Ther* 1:5.
  18. Inoue T, M Sugiyama, H Hattori, H Wakita, T Wakabayashi and M Ueda. (2013). Stem cells from human exfoliated deciduous tooth-derived conditioned medium enhance recovery of focal cerebral ischemia in rats. *Tissue Eng Part A* 19:24–29.
  19. Taghipour Z, K Karbalaie, A Kiani, A Niapour, H Bahrmanian, MH Nasr-Esfahani and H Baharvand. (2012). Transplantation of undifferentiated and induced human exfoliated deciduous teeth-derived stem cells promote functional recovery of rat spinal cord contusion injury model. *Stem Cells Dev* 21:1794–1802.
  20. Sugimura-Wakayama Y, W Katagiri, M Osugi, T Kawai, K Ogata, K Sakaguchi and H Hibi. (2015). Peripheral nerve regeneration by secretomes of stem cells from human exfoliated deciduous teeth. *Stem Cells Dev* 24:2687–2699.
  21. Sugiyama M, K Iohara, H Wakita, H Hattori, M Ueda, K Matsushita and M Nakashima. (2011). Dental pulp-derived CD31(–)/CD146(–) side population stem/progenitor cells enhance recovery of focal cerebral ischemia in rats. *Tissue Eng Part A* 17:1303–1311.
  22. Shimojima C, H Takeuchi, S Jin, B Parajuli, H Hattori, A Suzumura, H Hibi, M Ueda and A Yamamoto. (2016). Conditioned medium from the stem cells of human exfoliated deciduous teeth ameliorates experimental autoimmune encephalomyelitis. *J Immunol* 196:4164–4171.
  23. Li X, J Xie, Y Zhai, T Fang, N Rao, S Hu, L Yang, Y Zhao, Y Wang and L Ge. (2019). Differentiation of stem cells from human exfoliated deciduous teeth into retinal photoreceptor-like cells and their sustainability in vivo. *Stem Cells Int* 2019:2562981.
  24. Wright AF, CF Chakarova, MM Abd El-Aziz and SS Bhattacharya. (2010). Photoreceptor degeneration: genetic and mechanistic dissection of a complex trait. *Nat Rev Genet* 11:273–284.
  25. Hong DH, BS Pawlyk, J Shang, MA Sandberg, EL Berson and T Li. (2000). A retinitis pigmentosa GTPase regulator (RPGR)-deficient mouse model for X-linked retinitis pigmentosa (RP3). *Proc Natl Acad Sci U S A* 97:3649–3654.
  26. Ding SLS, S Kumar and PL Mok. (2017). Cellular reparative mechanisms of mesenchymal stem cells for retinal diseases. *Int J Mol Sci* 18:pii:E1406.
  27. Inoue Y, A Iriyama, S Ueno, H Takahashi, M Kondo, Y Tamaki, M Araie and Y Yanagi. (2007). Subretinal transplantation of bone marrow mesenchymal stem cells delays retinal degeneration in the RCS rat model of retinal degeneration. *Exp Eye Res* 85:234–241.
  28. Tzameret A, I Sher, M Belkin, AJ Treves, A Meir, A Nagler, H Levkovitch-Verbin, Y Rotenstreich and AS Solomon. (2015). Epiretinal transplantation of human bone marrow mesenchymal stem cells rescues retinal and vision function in a rat model of retinal degeneration. *Stem Cell Res* 15:387–394.
  29. Tzameret A, I Sher, M Belkin, AJ Treves, A Meir, A Nagler, H Levkovitch-Verbin, I Barshack, M Rosner and Y Rotenstreich. (2014). Transplantation of human bone marrow mesenchymal stem cells as a thin subretinal layer ameliorates retinal degeneration in a rat model of retinal dystrophy. *Exp Eye Res* 118:135–144.
  30. Lu B, S Wang, S Girman, T McGill, V Ragaglia and R Lund. (2010). Human adult bone marrow-derived somatic cells rescue vision in a rodent model of retinal degeneration. *Exp Eye Res* 91:449–455.
  31. Athanasiou D, M Aguila, J Bellingham, W Li, C McCulley, PJ Reeves and ME Cheetham. (2018). The molecular and cellular basis of rhodopsin retinitis pigmentosa reveals potential strategies for therapy. *Prog Retin Eye Res* 62:1–23.
  32. Liu X, Y Zhang, Y He, J Zhao and G Su. (2015). Progress in histopathologic and pathogenetic research in a retinitis pigmentosa model. *Histol Histopathol* 30:771–779.
  33. Maguire AM, F Simonelli, EA Pierce, EN Pugh, Jr., F Mingozzi, J Bennicelli, S Banfi, KA Marshall, F Testa, et al. (2008). Safety and efficacy of gene transfer for Leber’s congenital amaurosis. *N Engl J Med* 358:2240–2248.
  34. Medawar PB. (1948). Immunity to homologous grafted skin. III. The fate of skin homographs transplanted to the brain, to subcutaneous tissue, and to the anterior chamber of the eye. *Br J Exp Pathol* 29:58–69.
  35. Streilein JW. (1995). Immunological non-responsiveness and acquisition of tolerance in relation to immune privilege in the eye. *Eye (Lond)* 9 (Pt 2):236–240.
  36. Marcus Frank HW. (1996). Cellular reactions at the lesion site after crushing of the rat optic nerve. *Glia* 16:227–240.
  37. Benhar I, A London and M Schwartz. (2012). The privileged immunity of immune privileged organs: the case of the eye. *Front Immunol* 3:296.
  38. Lohan P, O Treacy, M Morcos, E Donohoe, Y O’Donoghue, AE Ryan, SJ Elliman, T Ritter and MD Griffin. (2018). Interspecies incompatibilities limit the immuno-

- modulatory effect of human mesenchymal stromal cells in the rat. *Stem Cells* 36:1210–1215.
39. Treacy O, L O'Flynn, AE Ryan, M Morcos, P Lohan, S Schu, M Wilk, G Fahy, MD Griffin, M Nosov and T Ritter. (2014). Mesenchymal stem cell therapy promotes corneal allograft survival in rats by local and systemic immunomodulation. *Am J Transplant* 14:2023–2036.
  40. Pan D, X Chang, M Xu, M Zhang, S Zhang, Y Wang, X Luo, J Xu, X Yang and X Sun. (2019). UMSC-derived exosomes promote retinal ganglion cells survival in a rat model of optic nerve crush. *J Chem Neuroanat* 96:134–139.
  41. Mead B and S Tomarev. (2017). Bone marrow-derived mesenchymal stem cells-derived exosomes promote survival of retinal ganglion cells through miRNA-dependent mechanisms. *Stem Cells Transl Med* 6:1273–1285.
  42. Johnson TV, NW DeKorver, VA Levasseur, A Osborne, A Tassoni, B Lorber, JP Heller, R Villasmil, ND Bull, KR Martin and SI Tomarev. (2014). Identification of retinal ganglion cell neuroprotection conferred by platelet-derived growth factor through analysis of the mesenchymal stem cell secretome. *Brain* 137 (Pt 2):503–519.
  43. Moisseiev E, JD Anderson, S Oltjen, M Goswami, RJ Zawadzki, JA Nolte and SS Park. (2017). Protective effect of intravitreal administration of exosomes derived from mesenchymal stem cells on retinal ischemia. *Curr Eye Res* 42:1358–1367.
  44. Bi B, R Schmitt, M Israilova, H Nishio and LG Cantley. (2007). Stromal cells protect against acute tubular injury via an endocrine effect. *J Am Soc Nephrol* 18:2486–2496.
  45. Xing L, R Cui, L Peng, J Ma, X Chen, RJ Xie and B Li. (2014). Mesenchymal stem cells, not conditioned medium, contribute to kidney repair after ischemia-reperfusion injury. *Stem Cells Res Ther* 5:101.
  46. Baraniak PR and TC McDevitt. (2010). Stem cell paracrine actions and tissue regeneration. *Regen Med* 5:121–143.
  47. Ferreira JR, GQ Teixeira, SG Santos, MA Barbosa, G Almeida-Porada and RM Goncalves. (2018). Mesenchymal stromal cell secretome: influencing therapeutic potential by cellular pre-conditioning. *Front Immunol* 9:2837.
  48. Mansoor H, HS Ong, AK Riau, TP Stanzel, JS Mehta and GH Yam. (2019). Current trends and future perspective of mesenchymal stem cells and exosomes in corneal diseases. *Int J Mol Sci* 20:pii:E2853.
  49. Lopez-Verrilli MA, A Caviedes, A Cabrera, S Sandoval, U Wyneken and M Khoury. (2016). Mesenchymal stem cell-derived exosomes from different sources selectively promote neuritic outgrowth. *Neuroscience* 320:129–139.
  50. Klingeborn M, WM Dismuke, C Bowes Rickman and WD Stamer. (2017). Roles of exosomes in the normal and diseased eye. *Prog Retin Eye Res* 59:158–177.

Address correspondence to:

*Li-Hong Ge*

*Department of Pediatric Dentistry*

*Peking University School and Hospital of Stomatology*

*No. 22, Zhongguancun South Avenue*

*Haidian*

*Beijing 100081*

*China*

*E-mail: gelihong0919@163.com*

Received for publication July 26, 2019

Accepted after revision September 20, 2019

Prepublished on Liebert Instant Online September 21, 2019